

The optoelectronic properties of group IV nanoparticles

Eimear Madden, Martijn A. Zwijnenburg*

Department of Chemistry, University College London, 20 Gordon
Street, London WC1H 0AJ, UK.

*Email: m.zwijnenburg@ucl.ac.uk

Supporting tables

Table S1 CNPs' Kohn-Sham (KS) highest-occupied molecular orbital (HOMO) and lowest-unoccupied molecular orbital (LUMO) energies and the corresponding KS HOMO-LUMO gap values as calculated using DFT and the highest occupied (-IP) and lowest unoccupied (-EA) quasiparticle states and the fundamental gap as calculated using evGW. All values in eV and obtained with the def2-SVP basis-set for structures optimised in the D_2 point group.

Nanoparticle	KS-HOMO	KS-LUMO	KS-Gap	-IP	-EA	Δf
C ₁₀ H ₁₆	-7.53	1.08	8.60	-9.91	3.33	13.24
C ₃₅ H ₃₆	-6.44	0.85	7.29	-8.12	2.81	10.93
C ₈₄ H ₆₄	-5.82	0.81	6.63	-7.10	2.58	9.68
C ₁₆₅ H ₁₀₀	-5.41	0.82	6.25	-6.44	2.50	8.91

Table S2 CNPs' Kohn-Sham (KS) highest-occupied molecular orbital (HOMO) and lowest-unoccupied molecular orbital (LUMO) energies and the corresponding KS HOMO-LUMO gap values as calculated using DFT and the highest occupied (-IP) and lowest unoccupied (-EA) quasiparticle states and the fundamental gap as calculated using evGW. All values in eV and obtained with the def2-TZVP basis-set for structures optimised in the D_2 point group.

Nanoparticle	KS-HOMO	KS-LUMO	KS-Gap	-IP	-EA	Δf
C ₁₀ H ₁₆	-7.52	0.58	8.10	-10.21	2.4	12.61
C ₃₅ H ₃₆	-6.40	0.34	6.74	-8.38	1.84	10.22

Table S3 CNPs' Kohn-Sham (KS) highest-occupied molecular orbital (HOMO) and lowest-unoccupied molecular orbital (LUMO) energies and the corresponding KS HOMO-LUMO gap values as calculated using DFT and the highest occupied ($-IP$) and lowest unoccupied ($-EA$) quasiparticle states and the fundamental gap as calculated using *evGW*. All values in eV and obtained with the *def2-QZVP* basis-set for structures optimised in the D_2 point group.

Nanoparticle	KS-HOMO	KS-LUMO	KS-Gap	-IP	-EA	Δf
$C_{10}H_{16}$	-7.52	0.20	7.72	-10.38	1.70	12.08

Table S4 CNPs' optical gap values as calculated using TDDFT and *evGW-BSE*. All values in eV and obtained with the *def2-SVP* basis-set for structures optimised in the D_2 point group.

Nanoparticle	ΔO (TDDFT)	ΔO (<i>evGW-BSE</i>)
$C_{10}H_{16}$	7.76	8.84
$C_{35}H_{36}$	6.64	7.65
$C_{84}H_{64}$	6.10	7.29
$C_{165}H_{100}$	5.79	6.70

Table S5 CNPs' oscillator strength of the lowest optically active state as calculated using TDDFT and *evGW-BSE*. All values in eV and obtained with the *def2-SVP* basis-set for structures optimised in the D_2 point group.

Nanoparticle	Oscillator strength (TDDFT)	Oscillator strength (<i>evGW-BSE</i>)
$C_{10}H_{16}$	0.00951	0.01518
$C_{35}H_{36}$	0.00015	0.00051
$C_{84}H_{64}$	0.00012	0.00030
$C_{165}H_{100}$	0.00025	0.00049

Table S6 CNPs' optical gap values as calculated using TDDFT and *evGW-BSE*. All values in eV and obtained with the *def2-TZVP* basis-set for structures optimised in the D_2 point group.

Nanoparticle	ΔO (TDDFT)	ΔO (<i>evGW-BSE</i>)
$C_{10}H_{16}$	7.23	8.31
$C_{35}H_{36}$	6.12	7.08

Table S7 CNPs' oscillator strength of the lowest optically active state as calculated using TDDFT and evGW-BSE. All values in eV and obtained with the def2-TZVP basis-set for structures optimised in the D_2 point group.

Nanoparticle	Oscillator strength (TDDFT)	Oscillator strength (evGW-BSE)
C ₁₀ H ₁₆	0.01350	0.01998
C ₃₅ H ₃₆	0.00039	0.00132

Table S8 CNPs' optical gap values as calculated using TDDFT and evGW-BSE. All values in eV and obtained with the def2-QZVP basis-set for structures optimised in the D_2 point group.

Nanoparticle	ΔO (TDDFT)	ΔO (evGW-BSE)
C ₁₀ H ₁₆	6.93	8.03
C ₃₅ H ₃₆	5.79	

Table S9 CNPs' highest occupied ($-IP$) and lowest unoccupied ($-EA$) quasiparticle states and fundamental gap as calculated using qsGW and the optical gap as calculated using qsGW-BSE. All values in eV and obtained with the def2-SVP basis-set for structures optimised in the D_2 point group.

Nanoparticle	$-IP$	$-EA$	Δf	Δo
C ₁₀ H ₁₆	-10.20	3.29	13.49	9.09
C ₃₅ H ₃₆	-8.46	2.77	11.23	7.94

Table S10 GeNPs' Kohn-Sham (KS) highest-occupied molecular orbital (HOMO) and lowest-unoccupied molecular orbital (LUMO) energies and the corresponding KS HOMO-LUMO gap values as calculated using DFT and the highest occupied ($-IP$) and lowest unoccupied ($-EA$) quasiparticle states and the fundamental gap as calculated using evGW. All values in eV and obtained with the def2-SVP basis-set for structures optimised in the D_2 point group.

Nanoparticle	KS-HOMO	KS-LUMO	KS-Gap	$-IP$	$-EA$	ΔF
Ge ₁₀ H ₁₆	-7.23	-0.65	6.57	-8.56	1.26	9.82
Ge ₃₅ H ₃₆	-6.40	-1.39	5.09	-7.25	0.15	7.52
Ge ₈₄ H ₆₄	-5.94	-1.86	4.08	-6.44	-0.66	5.78
Ge ₁₆₅ H ₁₀₀	-5.64	-2.11	3.52	-	-	-

Table S11 GeNPs' Kohn-Sham (KS) highest-occupied molecular orbital (HOMO) and lowest-unoccupied molecular orbital (LUMO) energies and the corresponding KS HOMO-LUMO gap values as calculated using DFT and the highest occupied ($-IP$) and lowest unoccupied ($-EA$) quasiparticle states and the fundamental gap as calculated using *evGW*. All values in eV and obtained with the *def2-TZVP* basis-set for structures optimised in the D_2 point group.

Nanoparticle	KS-HOMO	KS-LUMO	KS-Gap	-IP	-EA	ΔF
Ge ₁₀ H ₁₆	-7.25	-0.83	6.42	-8.90	0.69	9.59
Ge ₃₅ H ₃₆	-6.43	-1.48	4.95	-7.62	-0.41	8.03

Table S12 GeNPs' Optical gap values as calculated using TDDFT and *evGW-BSE*. All values in eV and obtained with the *def2-SVP* basis-set for structures optimised in the D_2 point group. The values in parentheses are the gap for the first bright excited-state for particles where the lowest excited-state is non-bright.

Nanoparticle	ΔO (TDDFT)	ΔO (<i>evGW-BSE</i>)
Ge ₁₀ H ₁₆	5.74 (5.90)	5.74 (6.23)
Ge ₃₅ H ₃₆	4.44	4.75 (4.82)
Ge ₈₄ H ₆₄	3.61	3.83
Ge ₁₆₅ H ₁₀₀	3.09	-

Table S13 GeNPs' oscillator strength of the lowest bright state as calculated using TDDFT and *evGW-BSE*. All values in eV and obtained with the *def2-SVP* basis-set for structures optimised in the D_2 point group. Asterisks have been added to those nanoparticles who have a non-bright lower excited state.

Nanoparticle	Oscillator Strength (TDDFT)	Oscillator Strength (<i>evGW-BSE</i>)
Ge ₁₀ H ₁₆	0.00685	0.01875
Ge ₃₅ H ₃₆ *	0.00543	0.00861
Ge ₈₄ H ₆₄	0.00012	0.00060
Ge ₁₆₅ H ₁₀₀	0.00003	-

Table S14 GeNPs' Optical gap values as calculated using TDDFT and evGW-BSE. All values in eV and obtained with the def2-TZVP basis-set for structures optimised in the D_2 point group. The values in parentheses are the gap for the first bright excited-state for particles where the lowest excited-state is non-bright.

Nanoparticle	ΔO (TDDFT)	ΔO (evGW-BSE)
Ge ₁₀ H ₁₆	5.63 (5.76)	5.64 (6.07)
Ge ₃₅ H ₃₆	4.40	4.66 (4.74)

Table S15 GeNPs' Optical gap values as calculated using TDDFT and evGW-BSE. All values in eV and obtained with the def2-QZVP basis-set for structures optimised in the D_2 point group. The values in parentheses are the gap for the first bright excited-state for particles where the lowest excited-state is non-bright.

Nanoparticle	ΔO (TDDFT)	ΔO (evGW-BSE)
Ge ₁₀ H ₁₆	5.57 (5.70)	5.57 (5.99)
Ge ₃₅ H ₃₆	4.36	

Table S16 GeNPs' highest occupied ($-IP$) and lowest unoccupied ($-EA$) quasiparticle states and fundamental gap as calculated using qsGW and the optical gap as calculated using qsGW-BSE. All values in eV and obtained with the def2-SVP basis-set for structures optimised in the D_2 point group. The values in parentheses are the gap for the first bright excited-state for particles where the lowest excited-state is non-bright.

Nanoparticle	$-IP$	$-EA$	Δf	Δo
Ge ₁₀ H ₁₆	-9.10	0.95	10.05	6.19 (6.52)
Ge ₃₅ H ₃₆	-7.75	-0.33	7.42	4.79

Supporting figures

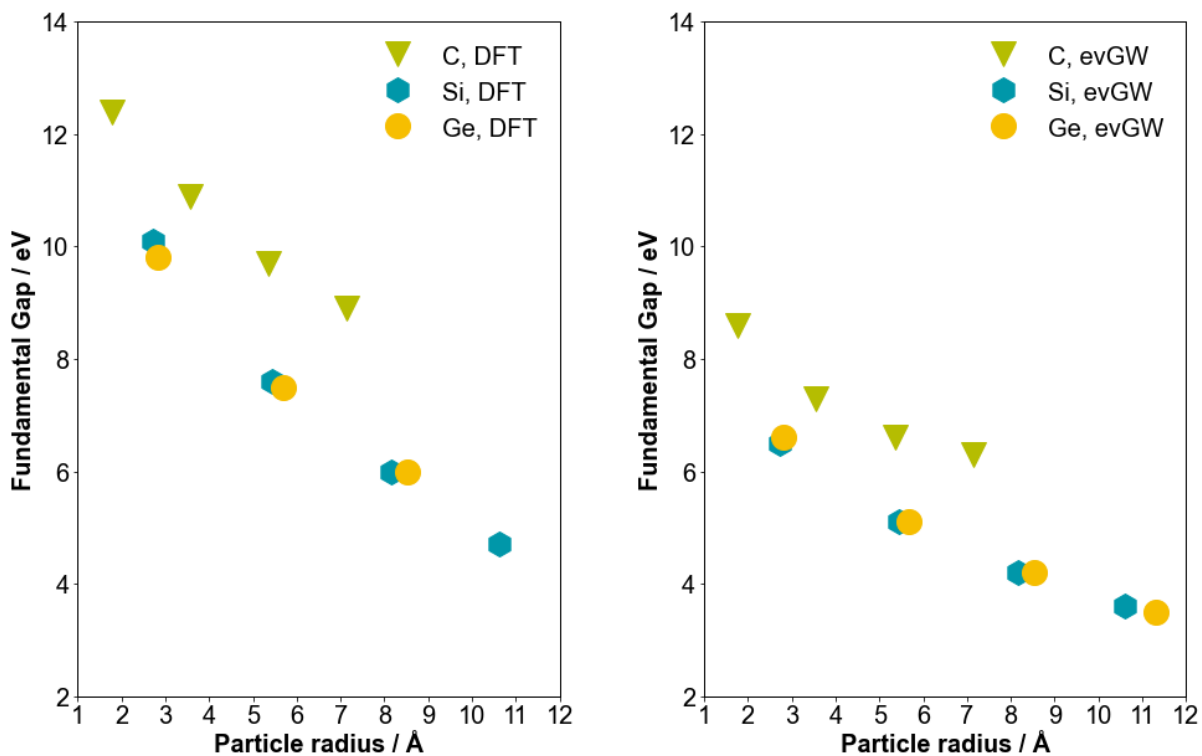


Fig. S1 Plot of fundamental gap versus particle radius for the different group 14 nanoparticles, where carbon is represented by green triangles, silicon is represented by blue hexagons and germanium is represented by yellow circles, calculated using DFT (right panel) and evGW (left panel). All calculations use/start from the B3LYP functional and use the def2-SVP basis-set and the D_2 point group.

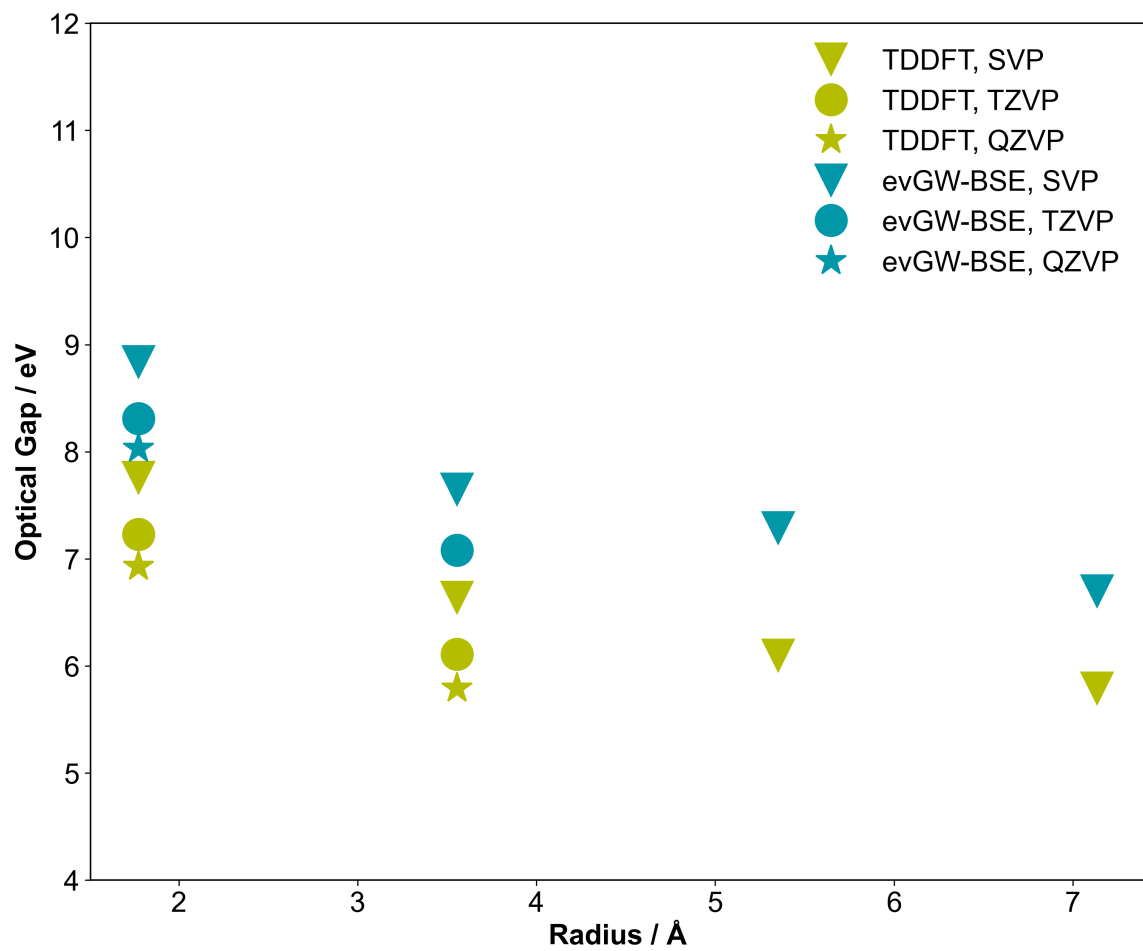


Fig. S2 Plot of optical gap versus particle radius for the carbon nanoparticles as calculated using the different basis-sets as calculated by TD-DFT and evGW-BSE. All calculations use/start from the B3LYP functional and the D_2 point group.

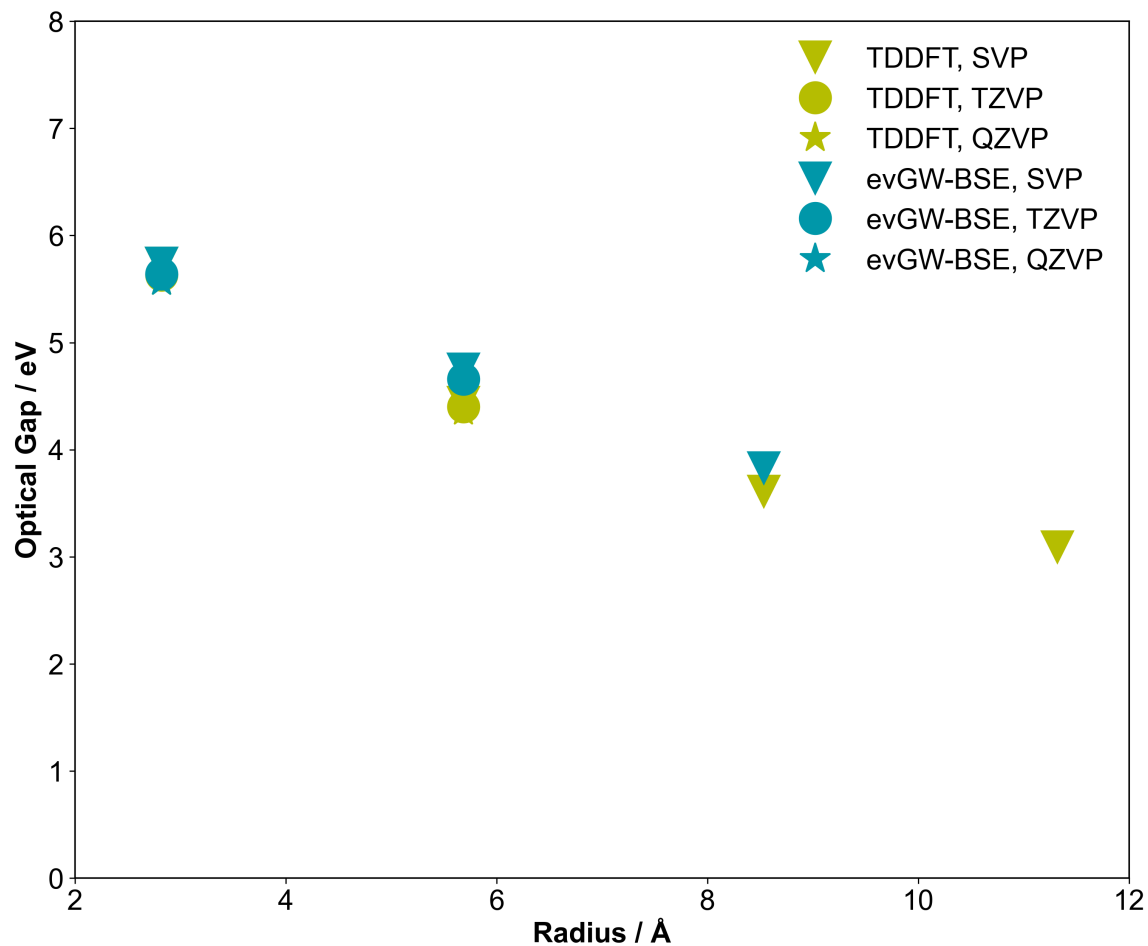


Fig. S3 Plot of optical gap versus particle radius for the germanium nanoparticles as calculated using the different basis-sets as calculated by TD-DFT and evGW-BSE. All calculations use/start from the B3LYP functional and the D_2 point group.

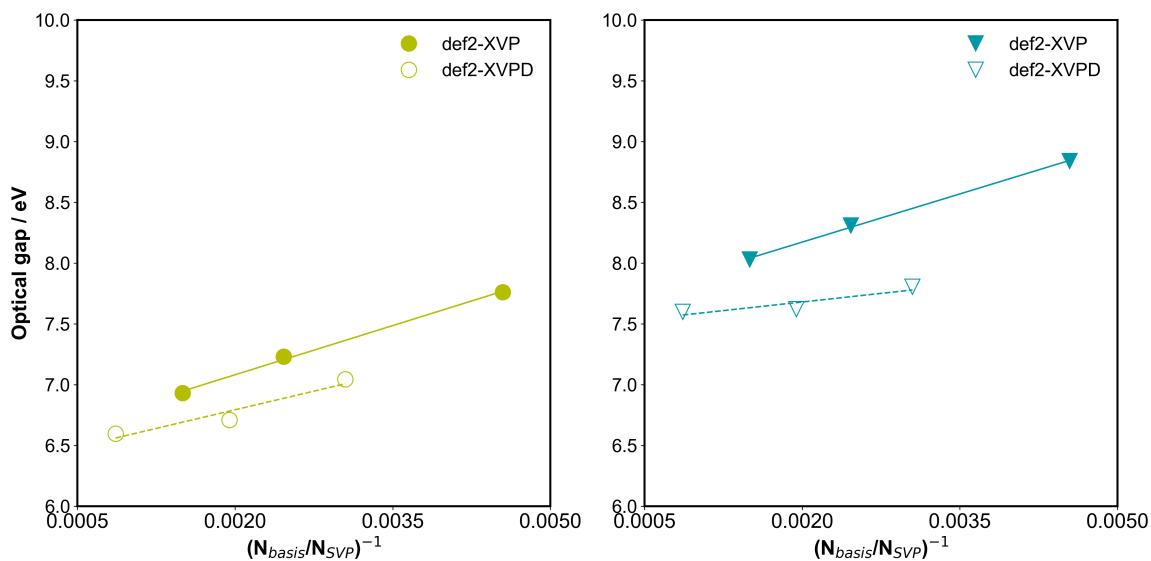


Fig. S4 Change in the predicted optical gap with increasing basis-set size when going from def2-SVP to def2-QZVP (closed symbols) and from def2-SVPD to def2-QZVPD for $C_{10}H_{16}$ calculated using TDDFT, D2, B3LYP (left panel) and evGW-BSE, D2, B3LYP (right panel). Dashed lines are linear fits to the predicted optical gap values.

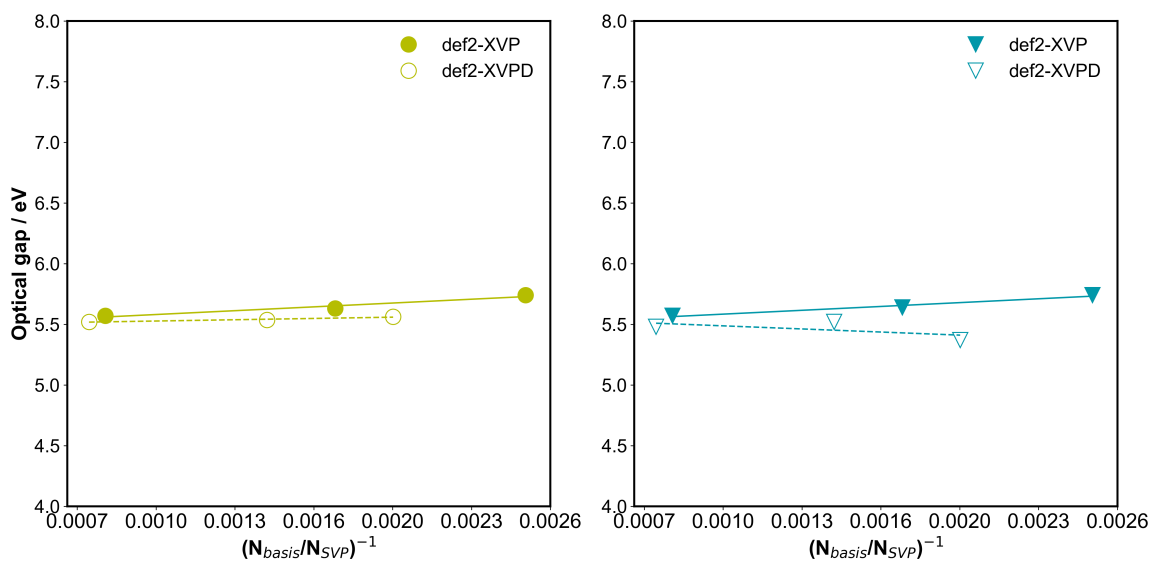


Fig. S5 Change in the predicted optical gap with increasing basis-set size when going from def2-SVP to def2-QZVP (closed symbols) and from def2-SVPD to def2-QZVPD for $Ge_{10}H_{16}$ calculated using TDDFT, D2, B3LYP (left panel) and evGW-BSE, D2, B3LYP (right panel). Dashed lines are linear fits to the predicted optical gap values.

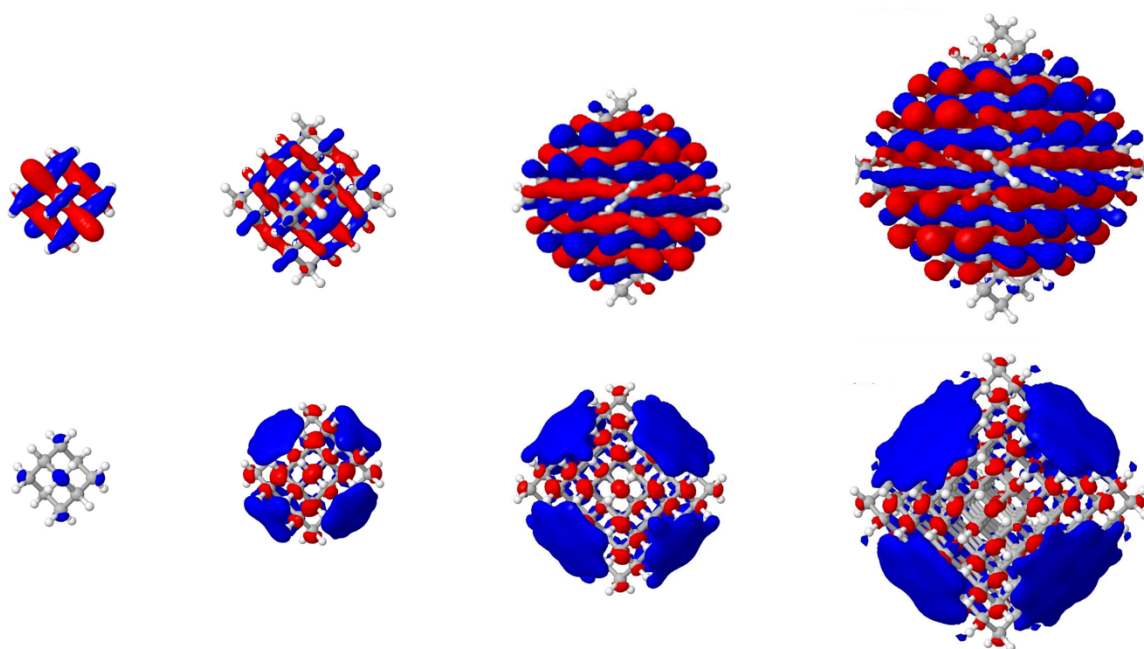


Fig. S6 Highest occupied (top) and lowest unoccupied (bottom) molecular orbitals of the four CNPs studied. From left to right: $C_{10}H_{16}$, $C_{35}H_{36}$, $C_{84}H_{64}$ and $C_{165}H_{100}$, where the phase of the orbitals is shown as red and blue, respectively. The highest occupied molecular orbital is triply degenerate and only one of the three degenerate orbitals is shown per particle. All results obtained using DFT, D_2 symmetry, B3LYP and the def2-SVP basis-set.

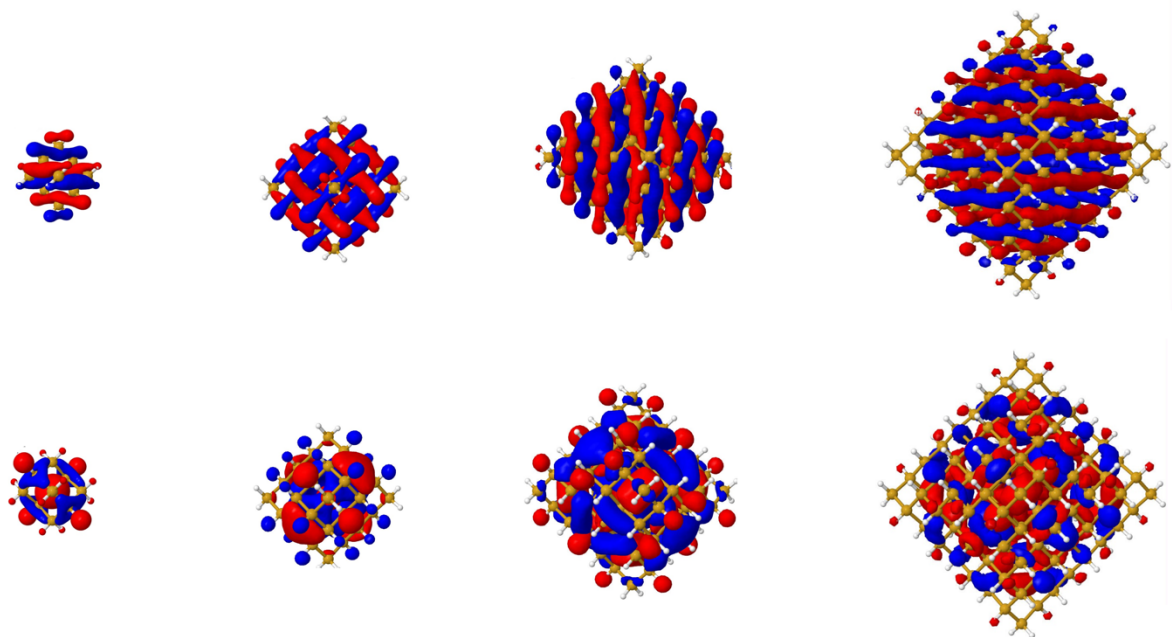


Fig. S7 Highest occupied (top) and lowest unoccupied (bottom) molecular orbitals of the four SiNPs studied. From left to right: $\text{Si}_{10}\text{H}_{16}$, $\text{Si}_{35}\text{H}_{36}$, $\text{Si}_{84}\text{H}_{64}$ and $\text{Si}_{165}\text{H}_{100}$, where the phase of the orbitals is shown as red and blue, respectively. The highest occupied molecular orbital is triply degenerate and only one of the three degenerate orbitals is shown per particle. All results obtained using DFT, D_2 symmetry, B3LYP and the def2-SVP basis-set.

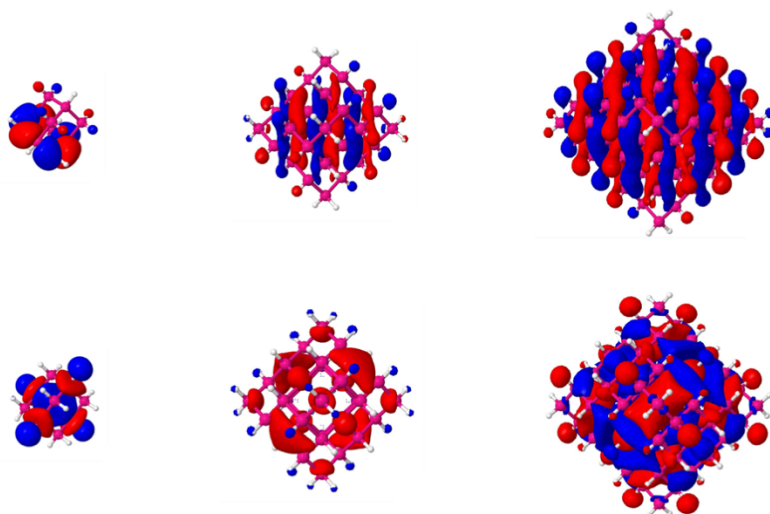


Fig S8. Highest occupied (top) and lowest unoccupied (bottom) molecular orbitals of the three GeNPs studied, $Ge_{10}H_{16}$ (left), $Ge_{35}H_{36}$ (centre) and $Ge_{84}H_{64}$ (right), where the phase of the orbitals is shown as red and blue, respectively. The highest occupied molecular orbital is triply degenerate and only one of the three degenerate orbitals is shown per particle. All results obtained using DFT, D_2 symmetry, B3LYP and the def2-SVP basis-set.

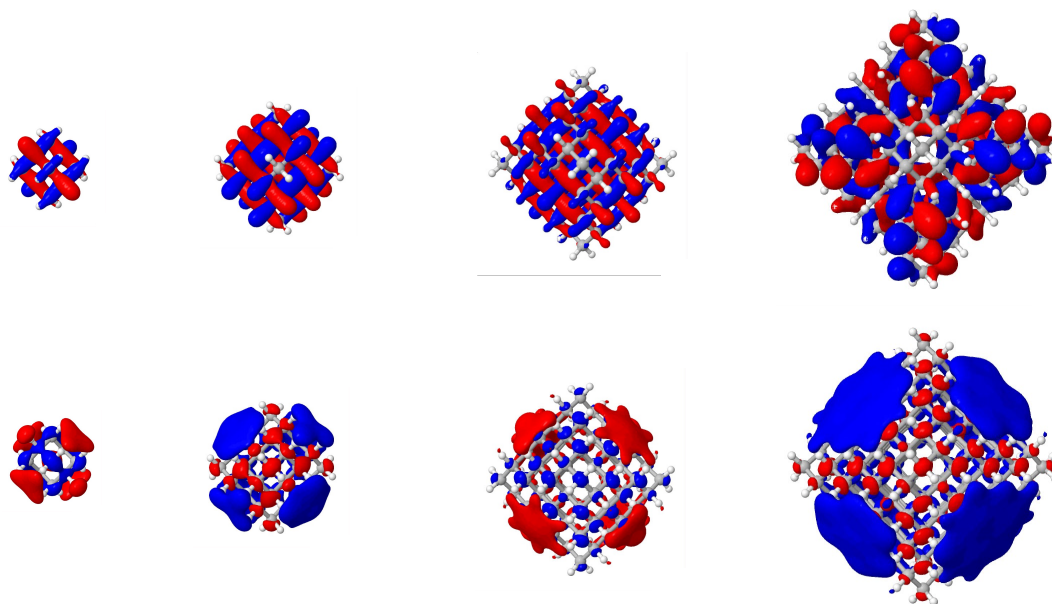


Fig. S9 Leading natural transition orbitals (NTOs) of the four CNPs studied. From left to right: $C_{10}H_{16}$, $C_{35}H_{36}$, $C_{84}H_{64}$ and $C_{165}H_{100}$, where the phase of the orbitals is shown as red and blue, respectively. Occupied orbitals are shown in the top row, virtual orbitals in the bottom row. The occupied orbital is triply degenerate and only one of the three degenerate orbitals is shown per particle. All results obtained using TDDFT, D_2 symmetry, B3LYP and the def2-SVP basis-set.

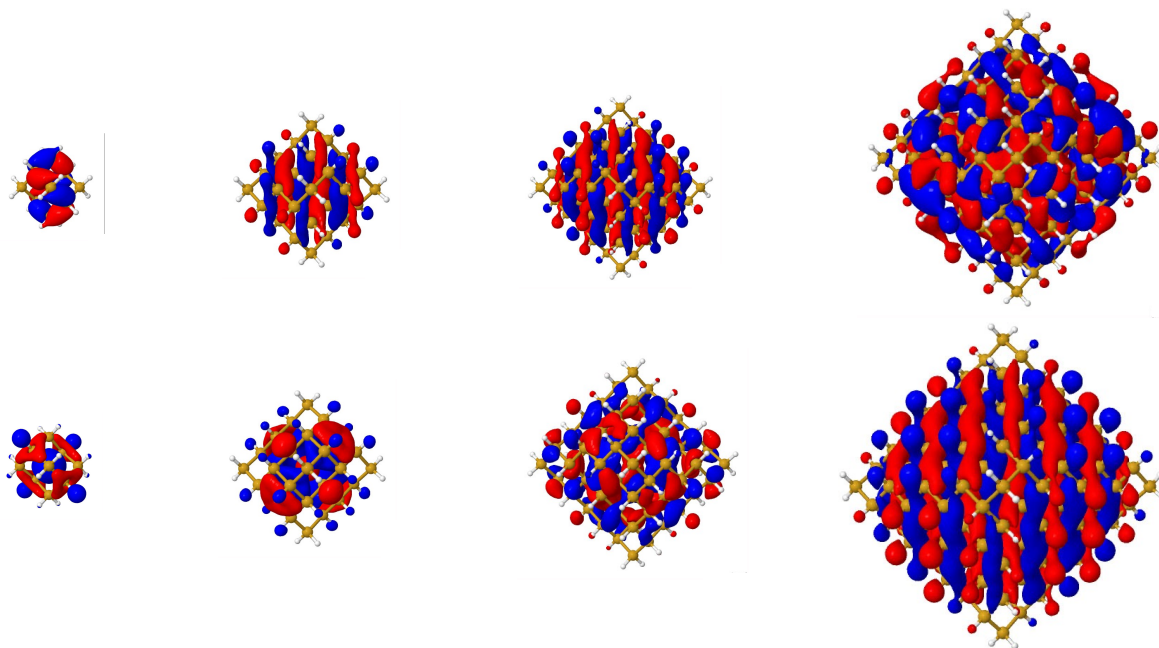


Fig. S10 Leading natural transition orbitals (NTOs) of the four SiNPs studied. From left to right: $\text{Si}_{10}\text{H}_{16}$, $\text{Si}_{35}\text{H}_{36}$, $\text{Si}_{84}\text{H}_{64}$ and $\text{Si}_{165}\text{H}_{100}$, where the phase of the orbitals is shown as red and blue, respectively. Occupied orbitals are shown in the top row, virtual orbitals in the bottom row. The occupied orbital is triply degenerate and only one of the three degenerate orbitals is shown per particle. All results obtained using TDDFT, D_2 symmetry, B3LYP and the def2-SVP basis-set.

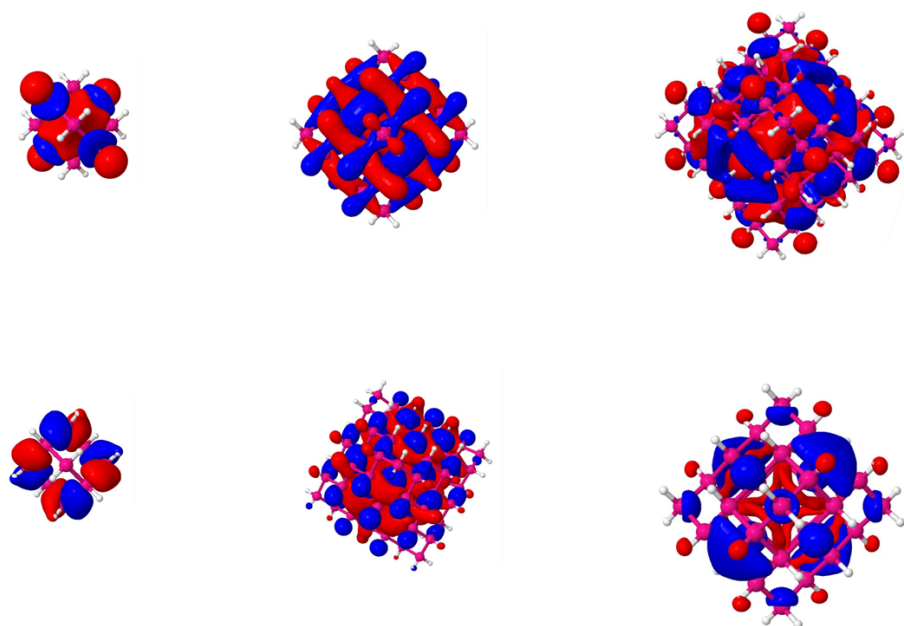


Fig. S11 Leading natural transition orbitals (NTOs) of three of the GeNPs studied. From left to right: $\text{Ge}_{10}\text{H}_{16}$, $\text{Ge}_{35}\text{H}_{36}$, and $\text{Ge}_{84}\text{H}_{64}$, where the phase of the orbitals is shown as red and blue, respectively. Occupied orbitals are shown in the top row, virtual orbitals in the bottom row. The occupied orbital is triply degenerate and only one of the three degenerate orbitals is shown per particle. All results obtained using TDDFT, D_2 symmetry, B3LYP and the def2-SVP basis-set.

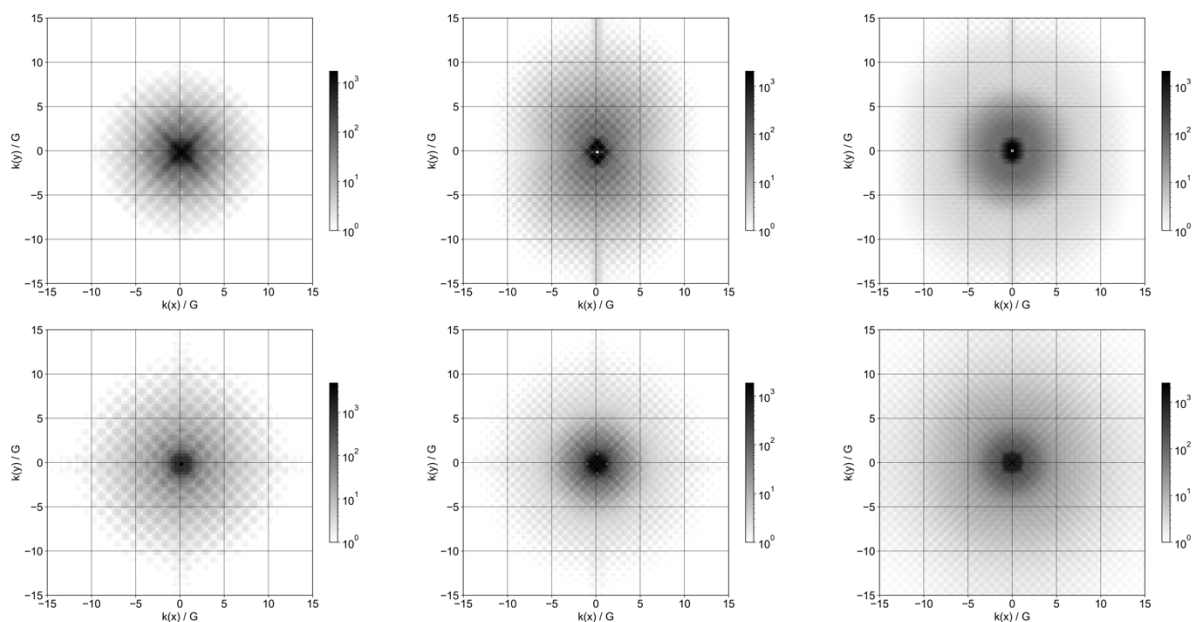


Fig. S12 Fourier transform of the leading natural transition orbitals (NTOs) as calculated using *evGW-BSE*, with *D2* symmetry, *B3LYP* and *def2-SVP*. Top; hole. Bottom; electron. $C_{10}H_{16}$ (left), $Si_{10}H_{16}$ (centre), $Ge_{10}H_{16}$ (right).

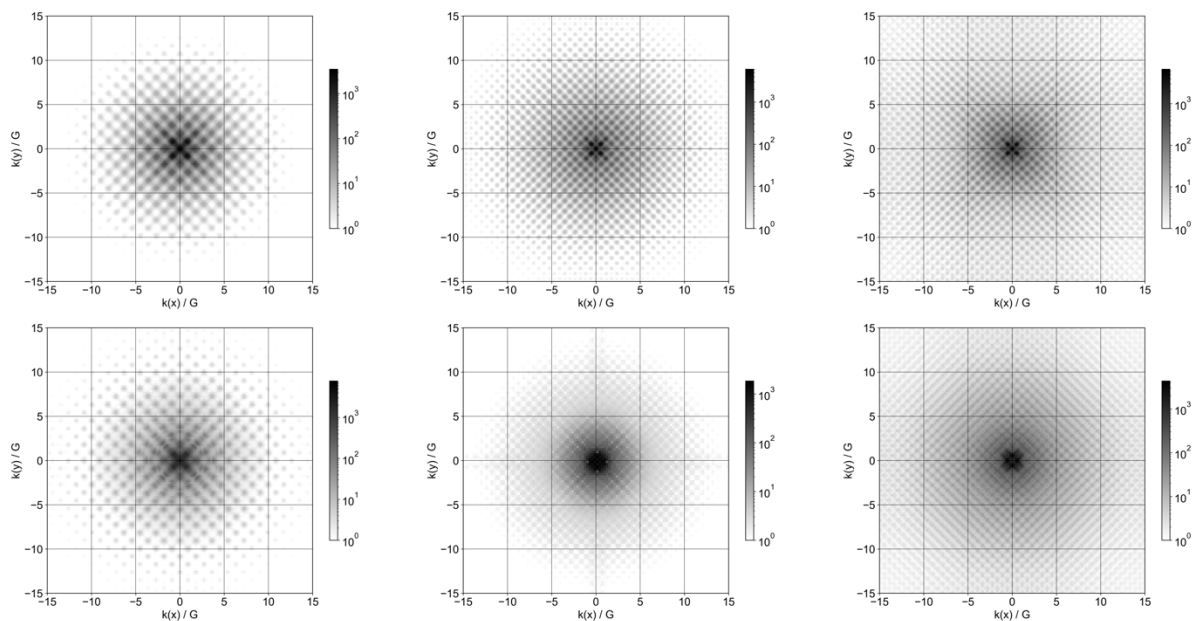


Fig. S13 Fourier transform of the leading natural transition orbitals (NTOs) as calculated using *evGW-BSE*, with *D2* symmetry, *B3LYP* and *def2-SVP*. Top; hole. Bottom; electron. $C_{84}H_{64}$ (left), $Si_{84}H_{64}$ (centre), $Ge_{84}H_{64}$ (right).